CHARACTERISATION OF GRAPHENE-ENHANCED CARBON-FIBRE/PEEK MANUFACTURED USING SPRAY-DEPOSITION AND LASER-ASSISTED AUTOMATED TAPE PLACEMENT (ATP)

Peter Kreider, Chris Stokes-Griffin, Christopher Leow, Silvano Sommacal, Paul Compston*

ARC Training Centre for Automated Manufacture of Advanced Composites, Australian National University, Canberra, ACT 2600, Australia.

*Corresponding author: peter.kreider@anu.edu.au

Abstract: *The inclusion of nanomaterials within fibre-reinforced polymer composites can enable novel high-performance structures, and graphene is one of the most promising candidate nanomaterials with a unique combination of exceptional mechanical, electrical, and thermal properties. Near-term graphene nanocomposites need to adopt both a scalable nanomaterial synthesis technique and a scalable method to integrate nanomaterials into composites during the manufacturing process. This work explores the spray-deposition of liquid phase exfoliated graphene for the interlaminar enhancement carbon-fibre reinforced polyether ether ketone (PEEK) composites. This approach enables spray-deposited nanomaterial thin films that can be incorporated directly into composites during advanced manufacturing processes such as laser-assisted automated tape placement, which we demonstrate here. Our preliminary investigations suggest that the presence of graphene can enhance the thermal history of the composite during manufacturing in addition to enhancing the properties of the manufactured composite material.*

Keywords: graphene; nanocomposite; laser-assisted automated tape placement

1. Introduction

Nanocomposites, composite materials including one or more components with dimensions on the nanoscale (1–100 nm), have demonstrated great potential to improve upon the already outstanding properties of engineered composites [1]. The combination of fibre reinforcement and high-performance nanomaterials could provide important advantages through increased thermal stability, electrical conductivity, toughness, and strength/stiffness. However, the interaction between the nanomaterials, the polymer matrix, and the reinforcing fibres could also have detrimental effects on the manufacturing process and on composite material properties, especially after traversing the many processing steps during manufacture. The fabrication technology and processing conditions used to manufacture composites can strongly affect material properties and structure on the nanoscale and, as a consequence, manufacturing composites and composite structures with retained nanostructure remains a challenge [1–3]. Traditional thermo-mechanical composite processing such as hot pressing and autoclaving creates an environment conducive to mechanisms like grain growth and aggregation, which have a tendency to eliminate or degrade the beneficial properties associated with nanostructure [2, 4]. Thus, modifications must be made to these manufacturing processes before they are capable of effectively enabling nanomaterial-enabled improvements at the macroscale [2, 4]. Alternatively, non-equilibrium processing techniques such as laser-assisted automated tape

  doi:10.5075/epfl-298799_978-2-9701614-0-0

placement (LATP) are excellent candidates for successful nanocomposite consolidation because they are rapid and avoid prolonged periods of time at high temperature and pressure [2].

Graphene-like materials have emerged as particularly promising nanomaterials for enhancing composites because they possess impressive intrinsic material properties such as strength, stiffness, and conductivity [5]. Their 2D nanoplatelet geometry allows for increased surface area to volume ratios and also enable self-assembly into laminated structures which is significant for imparting anisotropic properties (e.g. fracture toughness, permeability) [6], and they are galvanically compatible with carbon fibres unlike metallic nanomaterials [7]. From a cost, scalability, and nanomaterial quality perspective the ideal technique for graphene generation is liquid-phase exfoliation (LPE) [8]. However, LPE-produced nanosuspensions must be further processed to generate graphene solids and so significant work is required to effectively integrate graphene from suspension into consolidated composite materials. Given the excellent scalability of LPE for graphene synthesis, it is likely that graphene and similar high-performance 2D nanomaterials will be commonly supplied in liquid-phase suspension; therefore, developing manufacturing and processing techniques that leverage those suspensions will be worthwhile.

Interlayer modifications (e.g. interlayers/interleaves or localised nanoadditions like spray deposition) have demonstrated capability for nano-enhanced composite materials [9–12]. However, it is still unclear to what extent the nano-addition to interfacial regions translates to an enhancement in full-scale consolidated parts. Limitations of these interlayer modification techniques can include the possibility of delamination between plies that have thick interlayer additions [12] and migration of nanomaterials away from ply surfaces after infusion/consolidation [13]. Spray deposition is a particular attractive option because it is a simple and effective way to add high-performance nanomaterials to precise locations within the composite, which is a scalable pathway for realistic, industrial-scale nanocomposites manufacturing [9, 10]. Our recent work has successfully demonstrated the enhancement of composite materials via the spray-deposition of nanosuspensions [14, 15]. Successful nanosuspension formulations would enable rapid generation of spray-templated, functionalised nanocoatings that can be incorporated directly into composites during manufacturing processes.

In this work, we investigate the integration of a nanomaterial spray-deposition system with LATP manufacturing, as visualised in Figure 1. Aqueous graphene nanosuspension synthesised using LPE methods was aerosolised and sprayed to generate graphene thin films on CF/PEEK. The resultant graphene thin films were characterised using both microscopy and surface profiling, while the chemical structure of graphene was chemically analysed using Raman spectroscopy. Finally, the interactions between graphene and the IR laser in LATP was studied in a simulated consolidation process.

  doi:10.5075/epfl-298799_978-2-9701614-0-0

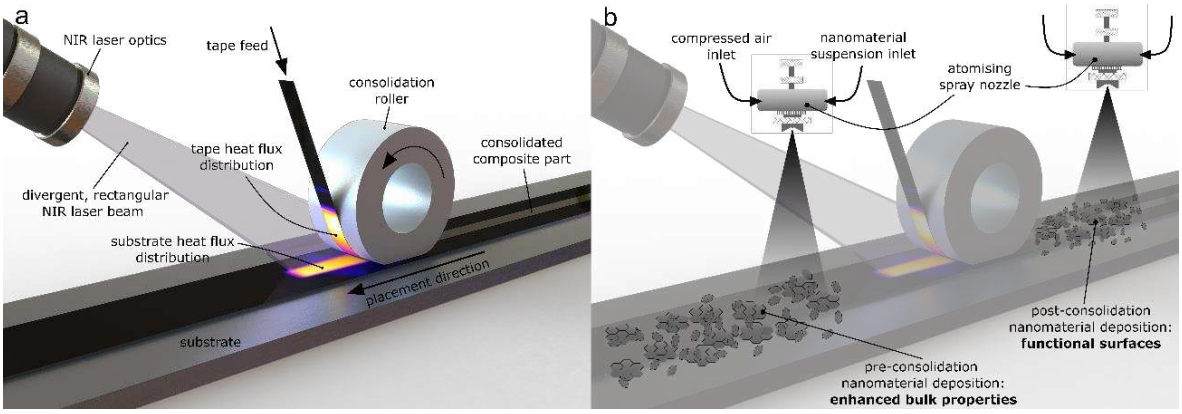

Figure 1. (a) The laser-assisted automated tape placement (LATP) concept based on commercial systems for thermoplastic-based carbon composites (adapted from [16]*) and (b) the LATP process with integrated nanomaterial spray-deposition either pre- or post-consolidation.*

2. Materials and Methods

Concentrated aqueous graphene suspension (1.5 wt% graphene, FlexeGRAPH Pty Ltd) was synthesised using surfactant-assisted liquid phase exfoliation in a continuous flow cell with a Q700 sonicator and 1" diameter probe tip attachment (Qsonica, USA) following the methodology developed by Notley [17]. Graphite was used as the feedstock material and non-ionic pluronic F68 surfactant (Sigma Aldrich) was continuously added for the first half of 240 hrs exfoliation time for a final graphite:F68 feed ratio of 1:1. 90x40 mm plies of carbon fibre (AS4)/polyether ether ketone (CF/PEEK) unidirectional tapes supplied by Toray Cetex (fibre volume fraction 59%) were used as the composite substrate material.

The graphene nanosuspensions were sprayed using a 30 mm diameter syringe filled with graphene suspension and placed in a NE-300 syringe pump (New Era Pump Systems Inc.). The suspension was fed into a flat fan air atomising nozzle (SUE15, Xinhou Industrial Co. Ltd) at a flow rate of 5 mL/min and aerosolised at 1 bar, as shown in Figure 2a. The substrate was placed at a distance of 300 mm and sprayed for 30 s before being placed on a hot plate at 50°C to dry. This process was repeated five times to generate the graphene thin film.

The CF/PEEK plies and spray-deposited graphene thin films on CF/PEEK (hereafter referred to as G-CF/PEEK) were characterised using optical microscopy and white light interferometry (WLI). Nikon Eclipse E200 microscope captured on a DS-Vi1 microscope camera (Nikon). Surface topography and roughness measurements were conducted on VEECO Wyko NT9100 Optical Profiling System using Vertical Scanning Interferometry (VSI) techniques. Five scans were taken at different locations on the sample for average root-mean-square roughness measurements.

Renishaw inVia confocal Raman microscope was used at a magnification of × 50 to chemically characterise graphene quality. Samples were exposed to a 532 nm wavelength laser at about 0.3 mW power with use of a 1200 mm−1 grating to isolate the signal and measurements were integrated over a period of 1 s with 10 accumulations to reduce signal to noise ratios.

For the LATP work, the optics on the laser tape placement head (AFPT GmbH) are supplied with a NIR laser beam (λ = 940–1100 nm) via fibre optic cables connected to a 4 kW laser (Laserline GmBH). A representative schematic of the LATP process is shown in Figure 1a. A 6-axis robot

  doi:10.5075/epfl-298799_978-2-9701614-0-0

arm (KUKA KR series) is used to control the position of the laser tape placement head and associated laser optics. To simulate graphene thin films being present during LATP consolidation, both CF/PEEK and G-CF/PEEK were irradiated with the AFPT tape placement head consolidation laser with a fixed laser power of 470 W and a tape placement head movement speed of 100 mm/s. The approximate dimensions of the laser spot projected on the sample are 55 mm and 23 mm in the process and transverse directions respectively, at a 60° angle of incidence.

3. Results and Discussion

Optical microscopy and WLI were used to characterise the quality and uniformity of the spray-deposited graphene thin film. The optical microscope images clearly show the carbon fibres and the presence of a light-scattering graphene thin film after spray deposition (Figure 2b, d). F68 surfactant is also present in the thin film but is not visually distinguishable from graphene. The natural gaps and channels in the CF/PEEK prepreg result in a surface roughness (R_{RMS} = 3.3 µm) as shown in Figure 2c. The aerosolisation and deposition of graphene nanosuspension covers the surface and fill in the gaps between fibres, resulting in a relatively smooth, conformal graphene thin film (R_{RMS} = 1.86 µm) on the surface of CF/PEEK (Fig 2e).

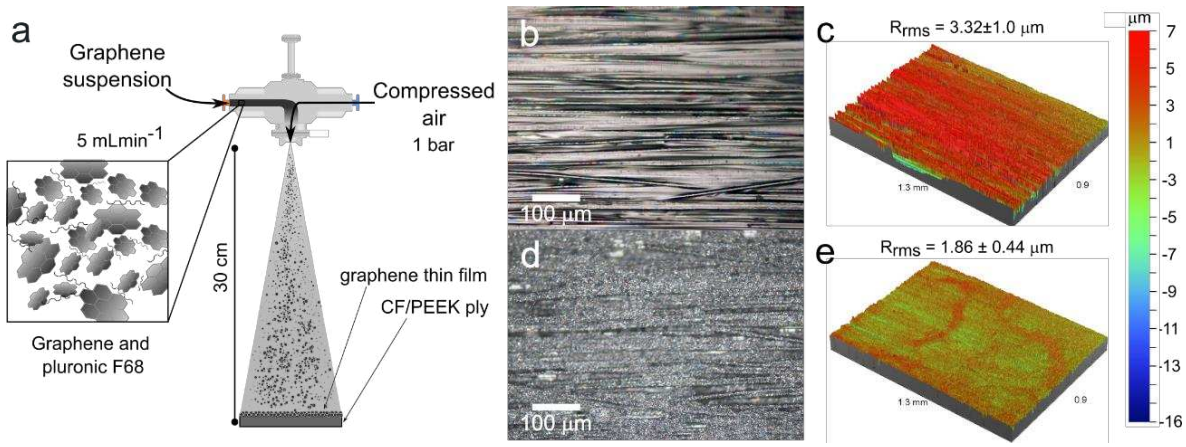

Figure 2. (a) Spray deposition process and parameters to aerosolise and deposit graphene suspension onto CF/PEEK composite plies. Graphical representation of graphene and pluronic F68 surfactant suspension inset. Optical microscope images (b ,d) and white light interferometry surface profiles (c,e) at 5x magnification of the CF/PEEK substrate and graphene thin film on CF/PEEK, respectively.

CF/PEEK and G-CF/PEEK materials were then subjected to IR laser heating in a simulated LATP manufacturing process. This simple process involved measuring the process parameter data both with and without graphene present pre-consolidation. The data from process monitoring for both CF/PEEK and G-CF/PEEK is shown in Figure 3. The in-situ process monitoring thermal camera is used to control the LATP consolidation parameters and is not directly equivalent to surface temperature due to process control algorithms and data processing. However, that surface temperature data is shown here as an indicator of how the graphene thin film affects heating rates and surface temperatures of both CF/PEEK and G-CF/PEEK materials.

  doi:10.5075/epfl-298799_978-2-9701614-0-0

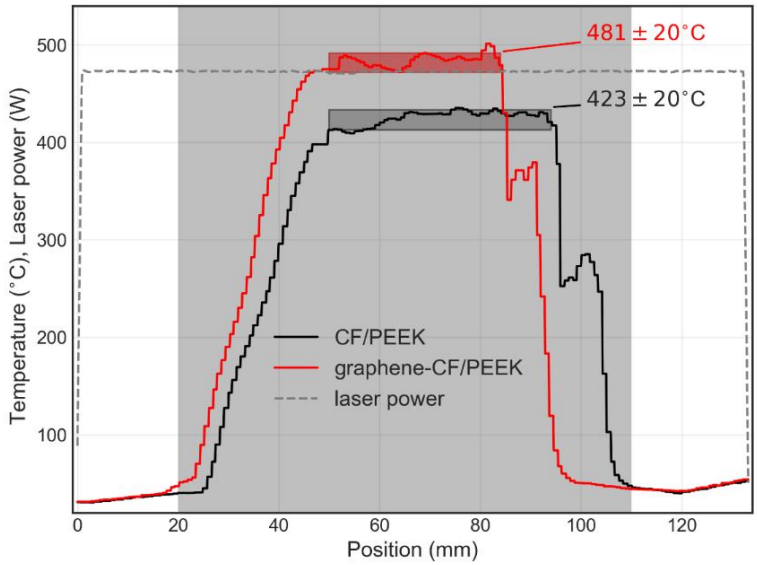

Figure 3. Process control thermal camera temperature and output laser power from the LATP placement head. The grey region represents the area covered by the 90 mm long prepreg plies as the head passes over the sample. The rectangular boxes indicate the 95% confidence interval for average steady-state surface temperature from the process thermal camera.

The G-CF/PEEK material heats up at a faster rate and to a greater temperature (481 ± 20 °C, 95% confidence) than neat CF/PEEK (423 ± 20 °C, 95% confidence). This is likely due to direct heating of graphene within the thin film, as exfoliated graphene can show a strong and broad absorption in the infrared region [18]. This suggests that the presence of graphene on the surface enhances absorption of the IR radiation, which could be beneficial to LATP manufacturing. Rapidly heating nanocarbon materials in air could negatively impact their properties. Therefore, the quality of graphene in the spray-deposited thin films before and after laser irradiation was assessed using Raman spectroscopy, shown in Figure 4.

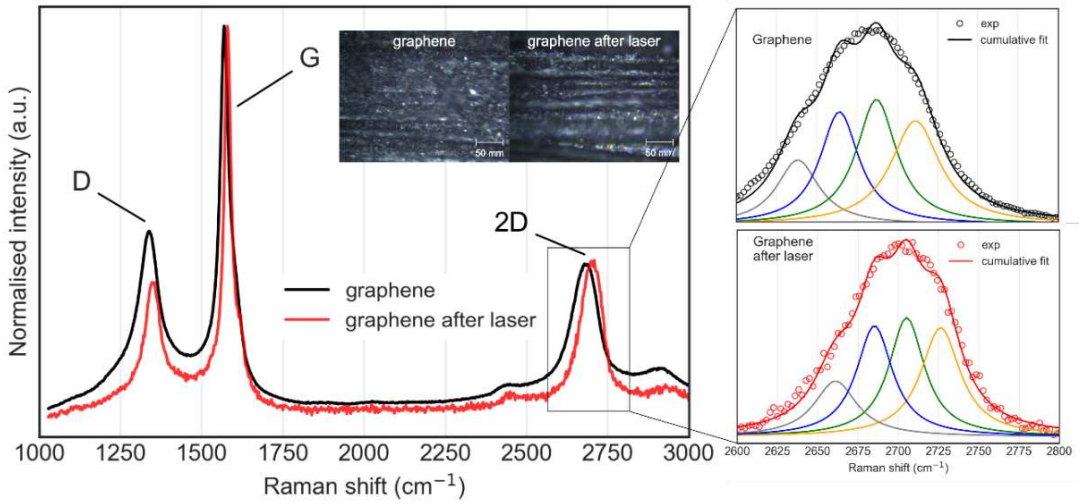

Figure 4. Raman spectra (microscope images from the Raman microscope inset) of the as-deposited graphene thin film on CF/PEEK and the same thin film after exposure to the LATP consolidation laser at 470 W power moving at 100 mm/s.

1044/1602 doi:10.5075/epfl-298799_978-2-9701614-0-0

The G peaks on both the as-deposited graphene thin film and the graphene thin film post-laser exposure can be fit with one Lorentzian curve at 1572 cm^{-1} before and 1581 cm^{-1} after laser exposure. The G peak is associated with the frequency of aromatic carbon rings stretching at ≈1580 cm^{-1} [19]. The D peak fit was centred at 1338 cm^{-1} before and 1351 cm^{-1} after laser exposure; the D peak is activated when defects are present in the graphene due to elastic scattering of charge carriers which only occurs when armchair edges are present [20, 21]. There is virtually no D' band present at 1620 cm^{-1} which suggests a low number of edge defects [20]. The D and D' peaks only occur when there is some level of disorder present in the graphene structure [20] and can be related to corrugations (e.g. ripples, wrinkles), topological defects (e.g. dislocations and grain boundaries), and atomic vacancies or adatoms (i.e. missing carbons, extra carbons, or carbon substitutions in the structure) [22]. The I_D/I_G peak intensity ratio increases with disorder and correlates with reduced charge carrier mobility [23]; the I_D/I_G ratio of the thin films in this work was equal to ≈0.5 before and ≈0.375 after laser exposure, typical for ultrasonic exfoliation synthesis [20, 24]. For context, the I_D/I_G ratio is ≈0 for pristine monolayer graphene and as high 1.31 for graphite [25]. The analysis of the D and G peaks in the spray-deposited graphene thin film are indicative of nanocrystalline carbon with few edge defects [20, 26]. The 2D peaks represent valance (π) and conduction (π*) bands where single layer graphene (SLG) can fitted using a single Lorentzian peak [27]. In bilayer and few-layer graphene (< 5 layers), electronic interactions between the layers cause the π and π* bands to split into four phonons which requires four Lorentzian bands to fit the 2D peak [28]. Four bands appeared at 2638, 2664, 2687, 2711 cm^{-1} before and 2661, 2685, 2705, 2726 cm^{-1} after. The 2D peak centres at 2682 cm^{-1} before and 2700 cm^{-1} after laser exposure. The intensity ratio of G to 2D (I_G/I_{2D}) both before and after laser exposure are both ~2.35, which falls in the appropriate range for exfoliated few layer graphene about 5 layers thick [29]. The full width half maximum of the 2D peak is 112 cm^{-1} before and 79 cm^{-1} after laser treatment which correlates to five or more graphene layers, but the 2D peak centres of ≈2700 cm^{-1} is indicative of 2–4 layer graphene [27]. The general blue shift of all peaks could be due to a laser-driven reduction in the number of layers in graphene, while a reduction in D band intensity could be due to a reduction of graphene edge defects. Blue shift could also arise because of the removal of surfactant after laser heating, which could change graphene surface strain. Collectively, the Raman spectroscopy analysis above suggests that the spray-deposited graphene thin films are high-quality exfoliated graphene roughly 4 to 7 layers thick [30]. After IR laser heating, the graphene Raman spectra presents a lower intensity D band, a slightly more pronounced 2D peak, and a general blue shift by about 13 cm^{-1}, which indicates laser-driven reduction in graphene edge defects and possible reduction in average graphene layer number. Overall, Raman analysis indicates that the graphene thin films are well suited to functionalising carbon fibre composites both before and after laser exposure.

4. Conclusion

The aerosolisation of aqueous graphene suspensions was able to generate smooth thin films on CF/PEEK prepreg tapes (RMS roughness 1.86 μm). The presence of this graphene thin film improved absorption of IR radiation from the LATP consolidation laser at fixed laser power (470 W), allowing surface temps to rise faster and to reach higher temperatures than CF/PEEK alone (481°C with vs 423°C without graphene). This suggests that a graphene thin film enables more efficient surface heating than neat CF/PEEK in LATP. Raman spectroscopy of the graphene thin films shows that high-quality multilayer graphene is present both before and after IR laser irradiation. The next step in this workflow is to consolidate a graphene-enhanced CF/PEEK

  doi:10.5075/epfl-298799_978-2-9701614-0-0

laminate using spray-deposition and LATP and to subsequently measure the mechanical, electrical, and thermal properties of that material. X-ray microCT scans will be also be used to explore the microstructure of graphene-modified CF/PEEK composites.

Acknowledgements

The authors acknowledge FlexeGRAPH for supplying the graphene suspension and J. Bradby for providing the facilities for Raman spectroscopy measurements. This project was conducted within the ARC Training Centre for Automated Manufacture of Advanced Composites (IC160100040), supported by the Commonwealth of Australia under the Australian Research Council's Industrial Transformation Research Program.

5. References

1. Njuguna J, Pielichowski K, Desai S (2008) Nanofiller-reinforced polymer nanocomposites. Polym Adv Technol 19:947–959
2. Viswanathan V, Laha T, Balani K, Agarwal A, Seal S (2006) Challenges and advances in nanocomposite processing techniques. Mater Sci Eng R Reports 54:121–285
3. Hussain F, Hojjati M, Okamoto M, Gorga RE (2006) Review article: Polymer-matrix nanocomposites, processing, manufacturing, and application: An overview. J Compos Mater 40:1511–1575
4. Zhang H, Peijs T (2020) Multifunctional composites based on hierarchical micro–nanostructures: design, manufacturing, properties, and applications. Fiber-Reinforced Nanocomposites Fundam Appl. https://doi.org/10.1016/b978-0-12-819904-6.00009-8
5. Mirabedini A, Ang A, Nikzad M, Fox B, Lau KT, Hameed N (2020) Evolving Strategies for Producing Multiscale Graphene-Enhanced Fiber-Reinforced Polymer Composites for Smart Structural Applications. Adv Sci. https://doi.org/10.1002/advs.201903501
6. Hu K, Kulkarni DD, Choi I, Tsukruk V V. (2014) Graphene-polymer nanocomposites for structural and functional applications. Prog Polym Sci 39:1934–1972
7. Kandare E, Khatibi AA, Yoo S, Wang R, Ma J, Olivier P, Gleizes N, Wang CH (2015) Improving the through-thickness thermal and electrical conductivity of carbon fibre/epoxy laminates by exploiting synergy between graphene and silver nano-inclusions. Compos Part A Appl Sci Manuf 69:72–82
8. Raccichini R, Varzi A, Passerini S, Scrosati B (2015) The role of graphene for electrochemical energy storage. Nat Mater 14:271–279
9. Zhang H, Liu Y, Kuwata M, Bilotti E, Peijs T (2015) Improved fracture toughness and integrated damage sensing capability by spray coated CNTs on carbon fibre prepreg. Compos Part A Appl Sci Manuf 70:102–110
10. Li Y, Zhang H, Liu Y, Wang H, Huang Z, Peijs T, Bilotti E (2018) Synergistic effects of spray-coated hybrid carbon nanoparticles for enhanced electrical and thermal surface conductivity of CFRP laminates. Compos Part A Appl Sci Manuf 105:9–18
11. Kumar V, Sharma S, Pathak A, Singh BP, Dhakate SR, Yokozeki T, Okada T, Ogasawara T (2019) Interleaved MWCNT buckypaper between CFRP laminates to improve through-thickness electrical conductivity and reducing lightning strike damage. Compos Struct 210:581–589
12. Kumar V, Yokozeki T, Okada T, Hirano Y, Goto T, Takahashi T, Ogasawara T (2018) Effect of through-thickness electrical conductivity of CFRPs on lightning strike damages. Compos Part A Appl Sci Manuf 114:429–438

13. Qin W, Vautard F, Drzal LT, Yu J (2015) Mechanical and electrical properties of carbon fiber composites with incorporation of graphene nanoplatelets at the fiber-matrix interphase. Compos Part B Eng 69:335–341
14. Leow C, Kreider PB, Notthoff C, Kluth P, Tricoli A, Compston P (2021) A graphene film interlayer for enhanced electrical conductivity in a carbon-fibre/PEEK composite. Funct Compos Mater. https://doi.org/10.1186/s42252-020-00015-9
15. Kreider PB, Cardew-Hall A, Sommacal S, Chadwick A, Hümbert S, Nowotny S, Nisbet D, Tricoli A, Compston P (2021) The effect of a superhydrophobic coating on moisture absorption and tensile strength of 3D-printed carbon-fibre/polyamide. Compos Part A Appl Sci Manuf 145:106380
16. Stokes-Griffin CM, Compston P (2015) A combined optical-thermal model for near-infrared laser heating of thermoplastic composites in an automated tape placement process. Compos Part A Appl Sci Manuf 75:104–115
17. Notley SM (2012) Highly concentrated aqueous suspensions of graphene through ultrasonic exfoliation with continuous surfactant addition. Langmuir 28:14110–14113
18. Quinn MDJ, Wang T, Al Kobaisi M, Craig VSJ, Notley SM (2018) PEO-PPO-PEO surfactant exfoliated graphene cyclodextrin drug carriers for photoresponsive release. Mater Chem Phys 205:154–163
19. Vázquez-Santos MB, Geissler E, László K, Rouzaud JN, Martínez-Alonso A, Tascón JMD (2012) Comparative XRD, Raman, and TEM study on graphitization of PBO-derived carbon fibers. J Phys Chem C 116:257–268
20. Childres I, Jauregui LA, Park W, Caoa H, Chena YP (2013) Raman spectroscopy of graphene and related materials. New Dev Phot Mater Res 403–418
21. Acik M, Chabal YJ (2011) Nature of graphene edges: A review. Jpn J Appl Phys. https://doi.org/10.1143/JJAP.50.070101
22. Yang G, Li L, Lee WB, Ng MC (2018) Structure of graphene and its disorders: a review. Sci Technol Adv Mater 19:613–648
23. Ma B, Rodriguez RD, Ruban A, Pavlov S, Sheremet E (2019) The correlation between electrical conductivity and second-order Raman modes of laser-reduced graphene oxide. Phys Chem Chem Phys 21:10125–10134
24. Saidin NU, Ying KK, Foo CT, Hazan R, Mahmoud ME (2019) Direct exfoliation of graphite and its Raman spectroscopic study. Mater Today Proc 7:798–802
25. Dubale AA, Su WN, Tamirat AG, Pan CJ, Aragaw BA, Chen HM, Chen CH, Hwang BJ (2014) The synergetic effect of graphene on Cu2O nanowire arrays as a highly efficient hydrogen evolution photocathode in water splitting. J Mater Chem A 2:18383–18397
26. Lucchese MM, Stavale F, Ferreira EHM, Vilani C, Moutinho MVO, Capaz RB, Achete CA, Jorio A (2010) Quantifying ion-induced defects and Raman relaxation length in graphene. Carbon N Y 48:1592–1597
27. Hao Y, et al., (2010) Probing layer number and stacking order of few-layer graphene by Raman Spectroscopy. Small 6:195–200
28. Ferrari AC, Meyer JC, Scardaci V, et al (2006) Raman spectrum of graphene and graphene layers. Phys Rev Lett 97:1–4
29. Gayathri S, Jayabal P, Kottaisamy M, Ramakrishnan V (2014) Synthesis of few layer graphene by direct exfoliation of graphite and a Raman spectroscopic study. AIP Adv. https://doi.org/10.1063/1.4866595
30. Kumar V, Kumar A, Lee DJ, Park SS (2021) Estimation of number of graphene layers using different methods. Materials (Basel). https://doi.org/10.3390/ma14164590